Critical span identification model with critical periods for dynamic thermal rating equipment arrangement

Yimin Yin[1], *Shihao* Wang[1] , *Qiang* Zhang[2], and *Mengxia* Wang[1,*]

[1]Key Laboratory of Power System Intelligent Dispatch and Control Ministry of Education (Shandong University), Jinan, Shandong Province, 250061, China
[2]Shandong Electric Power Dispatching and Control Center, Jinan, Shandong Province, 250022, China

Abstract. Compared with static thermal rating (STR), dynamic thermal rating (DTR) technology can explore the potential current-carrying capacity of overhead lines and bring considerable economic benefits. Considering that there are many spans of the overhead line, it is uneconomical to arrange equipment on each span. It is necessary to balance the investment cost and evaluation accuracy, and select the spans that can represent the current-carrying capacity of the whole line for monitoring. These spans are called 'critical spans'. The critical spans are the spans with low DTR, and these current-carrying capacities limit the increase of the current of the whole line, which are most likely to exceed the current limit. The current along the overhead line is constantly fluctuating, and it is possible to exceed the current limit only when the current is large and exceeds the STR. In this paper, the periods are filtered before selecting the critical spans, which are called the 'critical periods'. Considering the above factors, this paper proposes a critical span identification model of overhead line considering the critical periods. While selecting the critical spans, it also ensures that each span does not violate the ground clearance.

1 Introduction

With the large-scale access of new energy to the power grid, the power generation and load of the power system increase rapidly. However, the power grid construction is relatively slow, the shortage of land resources and the implementation of energy conservation and emission reduction political issues will further aggravate the lag of power grid construction, resulting in the lack of power grid transmission capacity[1]. Therefore, it is urgent to explore the potential current-carrying capability of the existing power grid. There are many reasons to limit the carrying capacity of transmission lines, including the use of static thermal rating (STR). STR is the conductor current-carrying capability formulated under the assumption that the worst meteorological conditions occur simultaneously (high ambient temperature, low wind speed, strong solar radiated, etc.).

* Corresponding author: wangmx@sdu.edu.cn

© The Authors, published by EDP Sciences. This is an open access article distributed under the terms of the Creative Commons Attribution License 4.0 (http://creativecommons.org/licenses/by/4.0/).

Although it is very convenient to use, it greatly underestimates the actual capacity of the transmission line[2,3]. In 1977, Davis, an American scholar, put forward the concept of dynamic thermal rating (DTR), which aims to calculate the transmission line ratings according to the results of meteorological measurements[4-6]. In most cases, DTR technology significantly improves the thermal rating calculation results, plays an important role in saving power grid construction investment and accepting new energy, and brings considerable economic benefits[7,8].

Based on the application requirements of DTR equipment, many researchers have studied the critical lines in power system[9-11]. After selecting the critical lines, it is necessary to identify the critical spans on these lines for the installation of DTR measurement equipment. The construction investment and maintenance cost of these equipment are large, so it is uneconomical to install many DTR measurement equipment along the line. The conventional placement position of DTR equipment is selected by evenly arranging the sensors along the transmission line. This placement method is called 'equidistant placement' (EDP) strategy[12]. Overhead lines usually traverse a large geographical area, and the meteorological conditions in these areas are quite different. Although this method is simple, it ignores the impact of meteorological conditions along the line on current-carrying capacity, and requires many sensors to play a role.

In order to improve the effectiveness of placement selection, it is necessary to model and analyze the placement position of DTR equipment, and these spans for installing sensors are called 'critical spans'. [13] considered that the span with the highest conductor temperature should be selected as the critical spans. A method to simulate the dynamic model of conductor temperature distribution of transmission line was proposed to identify the critical span by reconstructing the conductor temperature distributions of all spans. [12] and [14] identify the critical span from the essence of current-carrying capacity, [12] proposed a heuristic method to identify the critical span. Based on historical meteorological data, this method took the minimum value of DTR of all spans as the DTR of the whole line, then calculated the Pearson's correlation coefficient between DTR of each span and the line DTR separately, took it as the standard for selecting critical spans. The required benchmark can be achieved by continuously adding the span with the largest Pearson's correlation coefficient to the critical span set. Based on the model in [12], [14] considered the mechanical state of the line, and introduced the sag model of conductor into the critical span identification model to ensure that all spans would not infringe the ground clearance.

Although the models proposed by [12] and [14] can identify the critical span from the essence of current-carrying capacity, the time distribution of line current is not considered. Due to the fluctuation of power load, the current along overhead line is also constantly changing, and may exceed the DTR in some periods, which are called 'critical period' in this paper. Therefore, it is necessary to pre-process the historical meteorological data, identify the critical spans on the basis of the critical periods, and reduce the impact of current-carrying capacity in non-critical periods on the results. Besides, the Pearson's correlation coefficient used in [12] and [14] do not fully represents the quality of the estimation of the thermal capacity under a few specific circumstances. The coefficient reflects the linear correlation between the two data sets. When the difference values between the current-carrying capacity sets of the critical spans and the whole line are equal, it is graphically represented that the line segments composed of the two sets are parallel. And the Pearson's correlation coefficient is the largest, but it is obvious that the span is not the critical span of the line. Therefore, this paper identifies the critical spans based on the statistical results.

The remainder of this paper is organized as follows. The basic models for the identification of critical span are described in Section 2. Section 3 introduces the identification method of critical span considering critical period. Section 4 analyzes the numerical results, and conclusions are drawn in Section 5.

2 Basic model

2.1 Calculation method of line current-carrying capacity

In the operating environment, the current-carrying capacity of overhead conductor is determined by its conductor temperature and meteorological environment. According to CIGRE standard[15], the heat balance equation (HBE) of the conductor can be expressed by:

$$m_l C_l \frac{\mathrm{d}T_s}{\mathrm{d}t} = I_l^2 r_l(T_s) + q_s^{solar} - q_s^{conv}(T_s) - q_s^{rad}(T_s)\,, \tag{1}$$

where m_lC_l is the product of the per unit length mass and specific heat capacity of the overhead line l (J/(kg·℃)); I_l is the current of the overhead line l (A) (assuming that the current along the line l is consistent); r_l is the per unit length resistance of the conductor of the overhead line l (Ω/m), considering the resistance-temperature effect, assuming that the resistance per unit length of the overhead line l at the reference temperature (T^{ref}) is r_l^{ref} (Ω/m) and the resistance-temperature coefficient is α, r_l can be expressed as: $r_l(T_k) = r_l^{ref}[1+\alpha(T_k - T^{ref})]$; T_s is the temperature of the overhead conductor on the span s (℃); q_s^{solar} is the per unit length solar heating of the overhead conductor on the span s (W/m); q_s^{conv} is the per unit length convective cooling of the overhead conductor on the span s (W/m); q_s^{rad} is the per unit length radiative cooling of the overhead conductor on the span s (W/m). q_s^{solar}, q_s^{conv} and q_s^{rad} on the right of equation (1) can be expressed as follows[15]:

$$q_s^{solar} = \beta Q_s^{se} D_l\,, \tag{2}$$

$$q_s^{conv} = A_s^{conv}\left(T_s - T_s^{amb}\right), \tag{3}$$

$$q_s^{rad}(t) = A_l^{rad}\left[\left(273+T_s\right)^4 - \left(273+T_s^{amb}\right)^4\right]. \tag{4}$$

In (2)-(4), β is the solar absorptivity of the conductor; Q_s^{se} is the solar radiated heat intensity of the overhead conductor on the span s (W/(m·K)); D_l is the diameter of the overhead line l (m); A_s^{conv} is the convective coefficient of the overhead conductor on the span s, which is mainly determined by the wind speed v_s (m/s) around the conductor and the angle between the wind and the axis of conductor δ_s (rad) (W/(m·K)); T_s^{amb} is the ambient temperature of the overhead conductor on the span s (℃); A_l^{rad} is the radiative heat transfer coefficient of the line l (W/(m·K^4)). The calculation method of the above parameters can refer to [15], which will not be repeated in this paper.

The current-carrying capability I_s^{max} on the span s can be expressed as (5) below by simple rearrangement of (1):

$$I_s^{max} = \sqrt{\frac{q_s^{conv}(T_s^{max}) + q_s^{rad}(T_s^{max}) - q_s^{solar}}{r_l(T_s^{max})}}\,, \tag{5}$$

where T_s^{max} is the maximum allowable temperature (MAT) on span s, which can be calculated in Section 3.

2.2 Conductor sag model

Due to the physical and mechanical characteristics of the overhead conductor, the changes of meteorological environment and conductor temperature will affect the sag of the spans. For a tensioning section with n^{sp} spans, the horizontal tensile stress of each span is calculated as a multiple of its initial tensile stress as shown in (6):

$$X_s^4\left(X_sK_{s,1}K_{s,2}-F_s\right)+(X_sK_{s,1}-\frac{E_lO_l}{H_s^{ini}})(X_s^2K_{s,3}+K_{s,4})\frac{a_s^2}{\left(L_s^{inc}\right)^2}=0,\ (s=1,\dots,n^{sp}), \quad (6)$$

where the abbreviations $K_{s,1},\dots, K_{s,4}$ and F_s can be obtained by referring to [16], and $K_{s,2}$ is related to the conductor temperature T_s of span s; X_s is stress coefficient of span s; E_l is the elasticity modulus of the line l (MPa); O_l is the conductor cross section of the line l (mm^2); H_s^{ini} is the installation tensile stress of the span s; a_s is the length of the span s; $L_s^{inc}=\sqrt{a_s^2+h_s^2}$, which is the inclined span length of the span s, and h_s is the height difference between the suspension supports of the two ends of the span s (m).

Due to the stress-strain effect of the conductor, the sag of the span s (L_s^{sag}) can be calculated:

$$L_s^{sag}=\frac{H_s^f}{\gamma_s}\left[\sqrt{1+\left(\frac{\gamma_sh_s}{2H_s^f\sinh\left(\frac{\gamma_sa_s}{2H_s^f}\right)}\right)^2}\cosh\left(\frac{\gamma_sa_s}{2H_s^f}\right)-\frac{h_s}{a_s}\operatorname{arsinh}\left(\frac{\gamma_sh_s}{2H_{ls}^f\sinh\left(\frac{\gamma_sa_s}{2H_s^f}\right)}\right)-1\right], \quad (7)$$

where $H_s^f=X_sH_s^{ini}O_l$, which represents the horizontal conductor tensile force of the span s (N); γ_s is the load of conductors on the span s (MPa/m).

2.3 Weather data

The meteorological conditions in Subsection 2.1 and 2.2 are correspond to the span one by one. To obtain these meteorological data, the inverse distance weighted (IDW) interpolation method is applied in this subsection:

$$W_s=\frac{\sum_{i=1}^{n^{sa}}W_i(1/d_i^2)}{\sum_{i=1}^{n^{sa}}(1/d_i^2)}, \quad (8)$$

where W_s is the estimated weather condition at span s; n^{sa} is the number of weather stations; W_i is the known weather data at weather station i; d_i is the distance between span s and weather station i.

3 Critical span identification model

Based on the Section 3, a critical span identification model is proposed in this section, which mainly has the following three phases.

3.1 Determination of MAT

The MAT of overhead lines is conventionally 70 ℃, which is determined by the thermal aging of overhead conductor, but the case of infringing the ground clearance will still occur in extreme weather conditions. Therefore, in this subsection, the MAT of each span under the limitation of mechanical conditions is calculated with the requirements of the clearance distance to the ground of each span. Finally, the MAT of span s T_s^{max} is determined based on considering the limitation of thermal aging and mechanical sates.

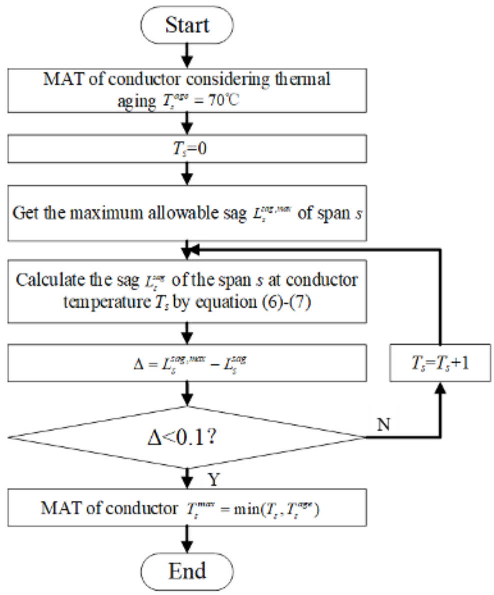

Fig. 1. Flowchart of determination of MAT.

The MAT T_s^{max} obtained from Fig. 1 not only meets the requirements of thermal aging limit, but also does not infringe the ground clearance. Combined with meteorological conditions, the current-carrying capacity I_s^{max} of each span can be calculated by equation (5).

3.2 Critical period selection method

The current of overhead line fluctuates with the load, which has strong daily regularity. The current exceeding the limit generally occurs at the period when the current is large and close to the DTR of the line. Therefore, these periods should be considered when identifying the critical spans. Considering that the DTR of the line is higher than STR in most cases[17], this subsection selects the periods with the current exceeds the STR, and identifies the critical spans in these critical periods.

3.3 Critical span identification method

After calculating the MAT in subsection 3.1 and selecting the critical periods in subsection 3.2, the critical spans can be identified by the following steps.

1) Initialization: The statistical benchmark B was set at 95%, the set composed of critical spans is $\boldsymbol{K}$ and initialized as an empty set, the set composed of all spans is $\boldsymbol{O}$

2) Weather data: Get the historical meteorological data of weather stations along the overhead line l, remove the unreasonable data, and interpolate through equation (8).

3) Current-carrying capacity series of the line l: Calculate the current-carrying capacity in critical periods of each span, and select the minimum value of current-carrying capacity at the same time as the current-carrying capacity of the line l to form the current-carrying capacity series ξ of line l.

4) Current-carrying capacity series of $\boldsymbol{\Gamma}$: $\boldsymbol{\Gamma}=\boldsymbol{Y}$**,** add the span s in $\boldsymbol{\tau}=\boldsymbol{O}-\boldsymbol{Y}$ into $\boldsymbol{\Gamma}$**,** take the minimum value of current-carrying capacity of all spans in $\boldsymbol{\Gamma}$ at the same time to form the series ω_s.

5) Calculation of statistical coefficient: Calculate the statistical coefficient ρ_s between the series ξ and the series ω_s. The statistical coefficient reflects the correlation of the two series. The larger the value of the coefficient is (the closer to 1), the current-carrying capacity of the critical span set is closer to the current-carrying capacity of the line *l*. The calculation method is shown in the following equation:

$$\rho_s = \frac{n_s^{\omega}}{n^{se}}, \ (n_s^{\omega} \leq n^{se}) \tag{9}$$

where n_s^{ω} is the number that the minimum value of DTR of the critical spans set are equal to the DTR of the whole line at the same time; n^{se} is the series dimension.

6) Determination of the critical span set ***Y***: After calculating the statistical coefficient of all sets $\boldsymbol{\Gamma}$ in step *4)* and *5)*, take the set $\boldsymbol{\Gamma}$ corresponding to the series ω_s with the highest coefficient ρ_{max} as the critical span set ***Y***.

7) Output: Repeat steps *4)-6)* until the statistical coefficient ρ_{max} reaches benchmark *B*, and output the critical span set ***Y*** and its statistical coefficient ρ_{max}.

The flowchart of the above steps is as follows:

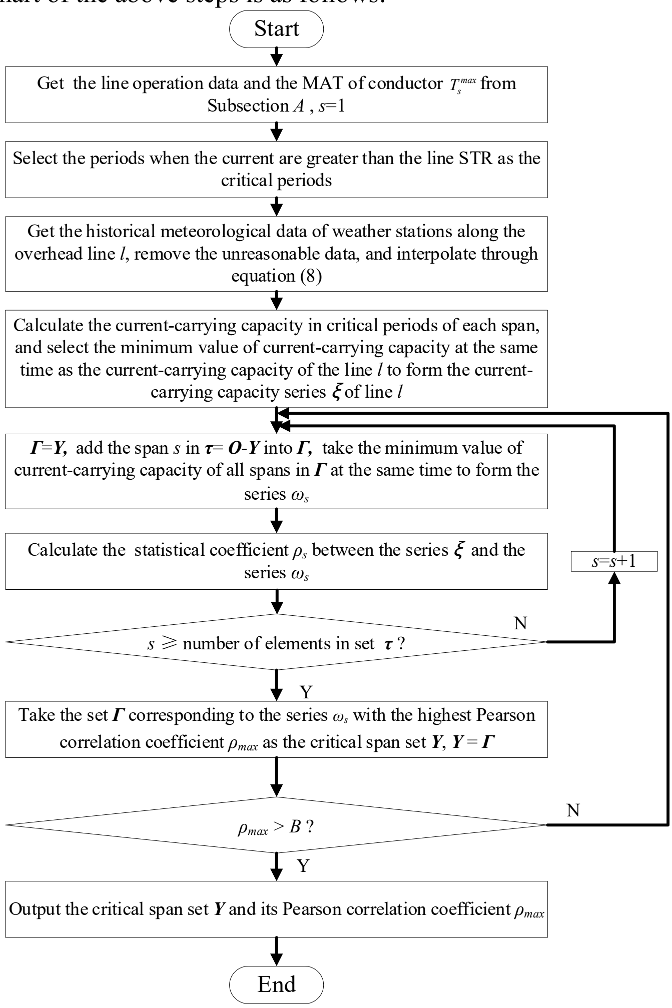

Fig. 2. Flowchart of critical span identification model.

The critical spans can be identified through the steps in Fig. 2.

4 Case study

The four lines included in this study are located in Shandong province, China. They are 16.86 km, 22.44 km, 32.24 km and 35.65 km long, respectively. The rated voltage of the system is 220kV, and the base capacity of the system is set to 100MVA. The conductor type of the overhead lines is ACSR 300/40 (the section areas of the aluminum part and the steel core are 300 mm^2 and 40 mm^2, respectively).

For comparison, a critical span identification model without considering the critical periods is also applied to the four lines.

4.1 Critical span identification model without considering the critical periods

This strategy does not consider the impact of different periods on the critical span identification model, which assumes that all periods play the same role in selecting the critical spans. The benchmark *B* was set at 85%, 90% and 95%, respectively. Table 1 shows the critical spans identification results of four lines by the method proposed in [14].

Table 1. Identification results with all periods.

Lines	Total Spans	*B*=0.85	*B*=0.9	*B*=0.95
		Critical spans	Critical spans	Critical spans
1	51	14	14,49	14,49,31
2	70	37	37,7	37,7,60,1,58
3	98	3,68	3,68,35,27	3,68,35,27,16,85,79
4	112	110,58,37	110,58,37,62,95,86	110,58,37,62,95,86,25,77, 12,2

Table 1 describes the identification results of critical spans of four lines. The Arabic numerals in the column of critical spans in Table 1 represent the order number of critical spans, for example, 14 represents the 14^{th} span of the line 1. The position of the spans represents the priority, and the front spans has higher priority than the rear spans.

In fact, as presented in Table 1, to reach a reasonable confidence value of 0.95 in the line 1 and line 2, 3 and 10 DTR measurement equipment are needed, respectively. The more spans of the line, the more DTR measurement equipment needed to be installed to reach the same confidence levels.

For different confidence levels, the critical spans identification results of the four lines are different. For a confidence level of 0.95, the difference in the number of the DTR measurement equipment is the largest.

4.2 Critical span identification model without considering the critical periods

By using the model proposed in this paper, the critical spans of the four lines are identified on the basis of selecting the critical periods. The identification results are shown in Table 2.

Table 2. Identification results with critical periods.

Lines	Total Spans	B=0.85	B=0.9	B=0.95
		Critical spans	Critical spans	Critical spans
1	51	14	14,31	14,31,49
2	70	7	7,60	7,60,37,1,58
3	98	35,3	35,3,79,62	35,3,79,62,27,85

Lines	Total Spans	B=0.85	B=0.9	B=0.95
		Critical spans	Critical spans	Critical spans
4	112	110,37,62	110,37,62,86	110,37,62,86,2,12,77,23

Table 2 describes the identification results of critical spans of four lines. Compared with Table 1, the identification results of critical spans of the four lines are different. The identification results in Table 2 show that the numbers of critical spans of line 1 and line 2 are the same, but the priority order of spans has changed. For example, after considering the critical periods, the priority of the 7th span of line 2 is higher than that of the 37th span.

For line 3 and line 4, not only the priority of the span has changed, but also the numbers of critical spans identified are less than that in Table 1. Because after considering the critical periods, the influence of the non-critical periods on the critical line identification result is reduced, and the identification efficiency is improved.

Compare the identification results of the two models of line 4, as shown in Fig. 3.

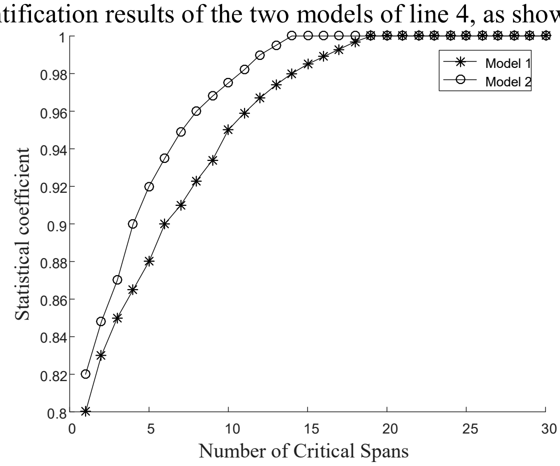

Fig. 3. Comparison of identification results of two models.

In Fig. 3, Model I is the critical span identification model without considering the critical periods and Model II is the critical span identification model considering the critical periods. From Fig. 3, after considering the critical periods, a few critical spans can reach a higher statistical coefficient than Model II, which proves the superiority of the critical span identification model considering the critical periods proposed in this paper.

5 Conclusion

In this paper, a critical span identification model based on critical periods selection is proposed. Through this model, the number and installation location of DTR measurement equipment can be provided based on historical meteorological information, and ensure that there will not infringe the ground clearance.

Different from other identification models, the model proposed in this paper considers the influence of critical periods on identification results. The critical periods in the historical data, that is, the periods in which the current are most likely to exceed the limit, are selected to reduce the impact of non-critical period on the identification results of critical spans. Through simulation analysis, the model proposed in this paper can achieve the same effect with selecting fewer critical spans, which reduces the installation and purchase cost of DTR measurement equipment.

References

1. Davis M W. A new thermal rating approach: the real time thermal rating system for strategic overhead conductor transmission lines–Part I: General description and justification of the real time thermal rating system *IEEE Trans Power Appar Syst* **96** pp 803–809 (1977)
2. Seppa O Clements M Damsgaard-Mikkelsen S et al. Application of real time thermal ratings for optimizing transmission line investment and operating decisions *CIGRE* Paper 22-301 (2000)
3. Cigre Brouchure. Increasing Capacity of Overhead Transmission Lines: Needs and Solutions (2010)
4. M W Davis A new thermal rating approach: the real time thermal rating system for strategic overhead conductor transmission lines Part I *IEEE Transactions on Power Apparatus and Systems* vol PAS-**96** 803-825 (1977)
5. M W Davis. A new thermal rating approach: the real time thermal rating system for strategic overhead conductor transmission lines Part II *IEEE Transactions on Power Apparatus and Systems* vol PAS-**97**:810-824 (1978)
6. M W Davis. A new thermal rating approach: the real time thermal rating system for strategic overhead conductor transmission lines Part III *IEEE Transactions on Power Apparatus and Systems* vol PAS-**97**:444-452 (1978)
7. Bishnu P Bhattarai, Jake P Gentle, Timothy McJunkin et al. Improvement of transmission line ampacity utilization by weather-based dynamic line rating *IEEE Trans Power Del* vol 33 no 4 pp 1853–1863 Aug (2018)
8. Hamid Shaker Mahmud Fotuhi-Firuzabad and Farrokh Aminifar. Fuzzy dynamic thermal rating of transmission lines *IEEE Trans Power Del* vol 27 no 4 pp 1885–1892 Oct (2012)
9. Z Huiping, M Jinbi, H Xiaoqing, B Liming, M Dongjuan and H Jie. A Critical Line Identification Method Based on Probabilistic Load Flow *2018 IEEE International Power Electronics and Application Conference and Exposition (PEAC)* pp 1-6 (2018)
10. Min Li, Lixiong Xu, Hui Gong, Zhaoou Song, Lijie Ding and Junyong Liu. Study on critical lines identification *Proceedings 2013 International Conference on Mechatronic Sciences Electric Engineering and Computer (MEC)* pp 3132-3135 (2013)
11. Y Cao, Y Zhang, C Guo, B Zhu and L Xu. Identification of power grid critical lines based on comprehensive transmission betweenness *2017 IEEE Power & Energy Society General Meeting* pp 1-5 (2017)
12. J Wan et al. Determination of critical span in real time using proper orthogonal decomposition *2013 Seventh International Conference on Sensing Technology (ICST)* pp 816-821 (2013)
13. M Matus et al Identification of Critical Spans for Monitoring Systems in Dynamic Thermal Rating *IEEE Transactions on Power Delivery* vol **27** no 2 pp 1002-1009
14. Cotton I and Teh J. Critical span identification model for dynamic thermal rating system placement *Iet Generation Transmission & Distribution* 9(16):2644-2652 (2015)
15. CIGRE. Guide for thermal rating calculations of overhead lines *CIGRE WG B2 43 Technical brochures 601* Dec (2014)
16. Kiessling F. Overhead power lines: planning, design, construction (2003)

17. X Jin, M Wang, M Cui, H Sun and M Yang Joint Probability Density Prediction for Multiperiod Thermal Ratings of Overhead Conductors *IEEE Transactions on Power Delivery* vol **36** no 5 pp 3022-3032